

Energy and Exergy Analysis of Flue Gas Waste Heat from Electrolytic Cells and Measures for Improving Its Grade

Jianjun Zhang¹, Ziqi Yu² and Wendong Qin³

1. Associate Researcher

Chinese Academy of Sciences - Guangzhou Institute of Energy Conversion, Guangzhou, China

2. Postgraduate Student

Shenyang University of Chemical Technology - School of Mechanical and Power Engineering, Shenyang, China

3. Assistant Engineer

Guangxi Baikuang Metallurgical Technology, Baise, China

Corresponding author: zhangjj@ms.giec.ac.cn

<https://doi.org/10.71659/icsoba2025-al062>

Abstract

During the aluminium electrolysis process, high-temperature gases such as carbon dioxide are produced. Under the negative pressure of the flue gas exhaust system, a large amount of air from the potroom enters through gaps in the hood, resulting in an increase in flue gas flow and a decrease of its temperature. The cell flue gas waste heat comes from the heat generated by the electrical current through the cell and from the oxidation of the carbon anodes. This paper estimates the gas and heat sources, flow rates, and waste heat amounts in the flue gas. Then, the useful work potential (exergy) of the waste heat is assessed. The higher the flue gas temperature, the greater the waste heat exergy and the higher the convertible energy. The current status of flue gas waste heat utilization is then presented.

Keywords: Aluminium electrolysis, Flue gas waste heat exergy analysis, Exergy improvement measures.

1. Introduction

Aluminium electrolysis production is an high temperature electrochemical process and belongs to the energy-intensive industry due to the high energy consumption per tonne of aluminium during the electrolysis process. Over 50 % of energy is lost in the form of waste heat [1]. The cell heat loss includes in particular the heat loss through flue gas, shell sidewall, cell hoods, and anode stems. Among these, shell sidewall and flue gas heat loss account for a large proportion. Sidewall heat loss is high in temperature but limited by spatial constraints, making the heat recovery difficult. Flue gas heat loss, however, accounts for approximately 36 % of the total heat loss, which is comparable to sidewall heat loss [2]. Since each cell is equipped with a complete gas collection system, recovery of flue gas heat is easier to achieve.

Currently, flue gas heat recovery faces challenges due to large flue gas flow, leading to low temperatures, poor quality of heat, high dust content, and a certain degree of corrosiveness in the gas. The return on investment for flue gas heat recovery is long, and companies are hesitant to invest [2]. Analysing the factors influencing flue gas flow and heat, taking into account the current status of flue gas heat utilization, and analysing the heat exergy, measures to improve waste heat exergy are proposed. Integrating AI analysis, factors affecting waste heat exergy can be combined to explore their internal relationships, find ways to improve the quality of flue gas heat, and stimulate smelters' interest in investing in flue gas heat recovery, thereby improving the overall energy utilization efficiency of the aluminium electrolysis process [1].

2. Determination of Cell Flue Gas Flow

In the aluminium electrolysis production process, the sources of flue gas captured by the cell exhaust system include gases produced during the aluminium electrolysis and the outside air drawn into the exhaust system through the cell gaps, such as those between the cell hoods, between the anode stem and the superstructure roof, etc. The flue cell gas flow rate can be measured using a Pitot tube flow meter installed on the cell main exhaust pipe through fixed measurement holes [3], or it can be estimated using mathematical models and empirical data from potrooms. The flue gas flow rate is related to the gaps in the hood. Different electrolytic cells have varying gap sizes in their hoods. For example, some older hoods have gaps over 2 cm between the hoods; this requires a large amount of gas to be drawn into the hoods to create negative pressure and prevent potroom emissions.

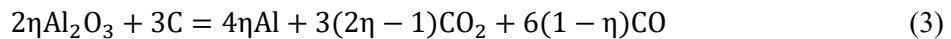
2.1 Process Gases Generated in Aluminium Electrolysis

In the electrolysis, the main gasses produced are CO₂ and CO, and in much smaller quantities CF₄ and C₂F₆ during anode effects. The amount of gas from the electrolytic process can be calculated from the mass balance in the reaction equations of the process, including auxiliary reactions of anode air oxidation and Boudouard reaction, also called carboxy reaction or CO₂ burn of anodes. The amount of process gas is small in the cell exhaust even with well-sealed hoods, typically less than 2 % as shown below.

The aluminium reduction reaction is given in Equation (1) and the reoxidation reactions in Equation (2):



Considering that the amount of reoxidation is current efficiency loss, the combination of the two equations gives the overall reaction, Equation (3):



where η is the current efficiency (fraction).

From this base reaction Equation (3), the following specific species production in mass can be deduced:

CO₂ production:

$$\frac{m_{\text{CO}_2}}{m_{\text{Al}}} = 1.2232877 \times \left(2 - \frac{1}{\eta}\right) \quad (4)$$

CO production from the re-oxidation reaction:

$$\frac{m_{\text{CO}}}{m_{\text{Al}}} = 1.5571492 \times \left(\frac{1}{\eta} - 1\right) \quad (5)$$

Electrolytic carbon consumption:

$$\frac{m_{\text{C}}}{m_{\text{Al}}} = \frac{0.3338615}{\eta} \quad (6)$$

Where m_i is the mass, in kg, of species $i = \text{Al}, \text{CO}_2, \text{CO}$ and C .

In addition to electrolysis Equation (3), the air burning of the anode generates CO_2 by reaction Equation (7), and Boudouard (carboxy) reaction generates CO by reaction Equation (8).



The consumption of carbon by these two reactions and a smaller contribution from carbon dust generation are called “excess carbon consumption”, which is the practical carbon consumption above the electrolytic consumption.

We will assume here that the carbon monoxide burns to CO_2 by the reaction:



An example for current efficiency of 94 % in a 400 kA cell:

- The mass of electrolytic carbon consumption is approximately 355 kg/t Al according to Equation (6).

According to Equations (4) and (5), it generates 1145 kg CO_2 /t Al and 99.4 kg CO/t Al.

- In industrial practice, the net carbon consumption is typically 410–420 kg/t Al. For the 415 kg/t Al median value, the resulting excess carbon consumption is $415 - 355 = 60$ kg/t Al.

For high anode current density cells with low anode cover thickness (western technologies), this may be divided into 50 % due to air burn (30 kg), 45 % due to Boudouard reaction (27 kg) and 5 % due to carbon dust generation.

For low anode current density with high anode cover (Chinese technologies), the carbon consumption due to anode oxidation is probably lower than the one due to Boudouard reaction. But energy-wise, this comes to the same heat generation in both cases if CO from Equation (5) burns to CO_2 under the hood.

Oxidation of 30 kg C/t Al generates 110 kg of CO_2 (Equation (7));

Burning of 27 kg C/t Al of carbon by Boudouard reaction generates 126 kg of CO/t Al (Equation (8)).

The total mass of these gasses is $1255 \text{ kg } \text{CO}_2 + 225 \text{ kg } \text{CO} = 1480 \text{ kg/t Al}$. On the other hand, if all CO (225 kg) burned into CO_2 , 354 kg of CO_2 would be generated. In that case, the total mass of process gas in the exhaust would be $1255 + 354 = 1609 \text{ kg } \text{CO}_2/\text{t Al}$

- The same cell produces 126.1 kg Al/h. Assuming gas exhaust rate of 8 000 Nm^3/h (N = Normal (Standard) temperature of 0 °C and pressure of 101.325 kPa, according to the ISO 10780:1994 standard [3]) gives 10 336 kg/h with a specific volume mass of 1.292 kg/Nm^3 (almost dry air). So the gas exhaust rate is 81 967 kg/t Al.

- Therefore, the process gasses make only $1480 \text{ to } 1609 / 81967 = 1.80 \text{ to } 1.96$ % weight of the total exhaust gas.

2.2 Flue Gas Volume from Air Intake Through Hood Gaps

To prevent harmful gases and dust under the hood from entering the potrooms, the exhaust system must maintain a minimum negative pressure under the cell superstructure hoods all along the cell length. The negative pressure in the exhaust system comes from two sources. One is the suction

force caused by the density difference between the flue gas under the cell hoods and the outside exhaust fan.

Assuming cell flue gas temperature of 200 °C, potroom temperature of 45 °C, and an exhaust duct at height of 2.7 m, the negative pressure at the duct inlet caused by the temperature difference between the inside and outside of the hoods can be estimated using Equation (10):

$$\Delta P = (\rho_f - \rho_0) \cdot g \cdot h \quad (10)$$

where:

- ΔP Negative pressure at the duct inlet, here -9.6 Pa resulting from the same formula
- g Acceleration of gravity, 9.81 m/s²
- h Height difference between the lower end of the hoods and the center of the exhaust system duct, 2.7 m
- ρ_0 Air density in the potroom, 1.109 kg/m³
- ρ_f Flue gas density inside the electrolytic cell, 0.746 kg/m³

The negative pressure caused by the temperature difference at the top of cell exhaust duct is -9.6 Pa, the negative pressure generated at the gap of the anode rod, which is only 1.35 m below the end of the exhaust pipe, is about -4.8 Pa, and the average negative pressure of the cell entire hood is about -2.4 Pa. These pressures alone are not sufficient to draw air into the cell in the whole length of the cell. At the tapping end of the cell, there will be air leakages from under the hood. Additional suction must be provided, and it is coming from the main exhaust fans.

With enough negative pressure, air from the potroom will be drawn into the cell through gaps in the hoods. The pressure drop Equation is given in Equation (11). The air velocity is given by the resulting Equation (12).

$$\Delta p = \frac{1}{2} \xi \rho_0 v^2 \quad (11)$$

$$v = \sqrt{\frac{2\Delta p}{\xi \rho_0}} \quad (12)$$

where:

- ξ Local pressure loss coefficient of the gaps between hoods with estimated value = 2
- ρ Air density in the potroom, 1.109 kg/m³ at 45 °C
- v Air speed through the gaps between the hoods, m/s

For gaps between hoods, the average negative pressure value is -2.4 Pa. With this pressure, Equation (12) gives an average inlet air velocity through the gaps between the hoods of 1.47 m/s. For a 420 kA cell, the hood length is 1.73 m, with 48 hoods in total, including both upper and lower gaps, the total gap length is about 123 m. Based on field observations, the average gap width between hoods is 5 mm. The gap area for a 420 kA cell is then 0.615 m², which gives an air intake of 0.615 × 1.47 × 3600 = 3 255 m³/h, which, converted to 150 °C operating conditions, corresponds to an exhaust volume of 3255 × (273+150)/(273+45) = 4 330 m³/h.

At the anode stem – ceiling plate interface, the under pressure is -4.8 Pa, which gives air velocity through the gap between the anode stem and the cell ceiling of 2.08 m/s ‘Equation (12). With multiple rods, the total gap length is 14.4 m, the average gap width is 7 mm, and the total area is

0.1008 m². This gives an additional flowrate of 755 m³/h at 45 °C, corresponding to 1004 m³/h at 150 °C.

In this example, the total flue gas in the cell exhaust duct, drawn into the cell by natural convection would be 5333 m³/h at 150 °C. However, this air cools the space inside the hood, the gas temperature becomes < 200 °C, and the negative pressures created by the thermal lift are smaller than the ones calculated above for 200 °C, due to a real density ρ_f slightly lower (Equation 10).

To ensure potroom air quality, the exhaust system's negative pressure, created by main exhaust fan, must be much higher than the natural convection value, e.g., on the order of -100 Pa [4], but this depends on the cell size, design of the gas intake in the superstructure [5], gas flowrate and open area in the hood. Lower open area of the hood requires less flowrate for capturing the emissions, but for a given flowrate the negative pressure inside the hood increases [4]. Typically, the total flue gas flowrate is around 10 000 Nm³/h in high amperage cells, of which process gases account for less than 2 % in weight. Consequently, gas temperature in the exhaust duct decreases [3], e.g., to < 150 °C, which is required for efficient dry scrubbing of alumina in Gas treatment Center (GTC). For effective heat recovery, high duct gas temperatures are required, i.e., lower gas flowrates, but this does not create problems with GTC since the heat recovery cools down the exhaust gas.

During anode replacement, typically two hoods are opened, giving an open ventilation area of about 2.482 m². This requires doubling the exhaust rate to almost stop the potroom emissions, and gas temperature in the duct will decrease drastically during anode change. Several cell technologies are equipped for double suction during anode change.

The calculations in this section are given to show the principles of cell ventilation. In practice today, CFD modelling of cell ventilation is used to design gas collection under the hood and exhaust system design.

3. Determination of Flue Gas Waste Heat

The heat taken out of the cell with flue gasses comes from the cell top, anode yokes and rods and the heat generated above the anode cover by anode air oxidation and CO burn, decreased by heat loss from the hoods, superstructure and anode rods above the hoods. The heat loss through the duct can be determined by measurements [4, 7] or simulations [4] or a combination of both. Heat loss through the duct is, Equation (13):

$$Q_D = \phi_m \cdot c_p \cdot (T_D - T_0) \quad (13)$$

In measurements, gas mass flowrate is obtained from volume flowrate Equation (14), which in turn is determined from the measurement of velocity profile v in the duct [3]:

$$\phi_m = \rho \cdot \phi_v = \rho \cdot v \cdot A \quad (14)$$

where:

Q_D	Duct heat loss, kW
ϕ_m	Gas mass flowrate, kg/s
c_p	Specific heat, J/kg·K
T_D	Duct gas temperature, °C
T_0	Temperature of air drawn into the hoods from the potroom, °C
ρ	Gas density, kg/m ³
ϕ_v	Volumetric flowrate, m ³ /s
A	Area of duct cross-section, m ²

v Gas velocity, m/s

Measurements and simulations of duct temperature and heat loss show that the duct temperature decreases with increased gas flowrate, but the heat loss increases with increased gas flowrate. An example is given in Figures 1 and 2. For heat recovery in the duct, these are contradicting results. For efficient heat recovery, we would like to have high gas temperature and high heat flow at the same time.

Cell top heat loss (from the anode cover yokes and rods) depends on cell design, amperage, cell size and on anode cover thickness. High anode current density cells (western technologies, 0.9–1.0 A/cm²) have low anode cover thickness (8–10 cm) and high top heat loss per unit area. Low anode current density cells (Chinese technologies, 0.7–0.8 A/cm²) have high anode cover (20 cm) and low heat loss per unit area. However, the total top heat loss and duct heat loss may be comparable at the same amperage since the low current density cell has much larger area. Figure 3 shows the dependence of top heat loss on anode cover thickness for a high anode current density cell, including anode yokes and anode rods inside the hood for fixed cell size [7]. The top heat loss depends also on duct flowrate [4]. In each particular case, the top heat loss must be determined, nowadays most likely by validated mathematical models [8] in order to know how much heat will be extracted through the duct.

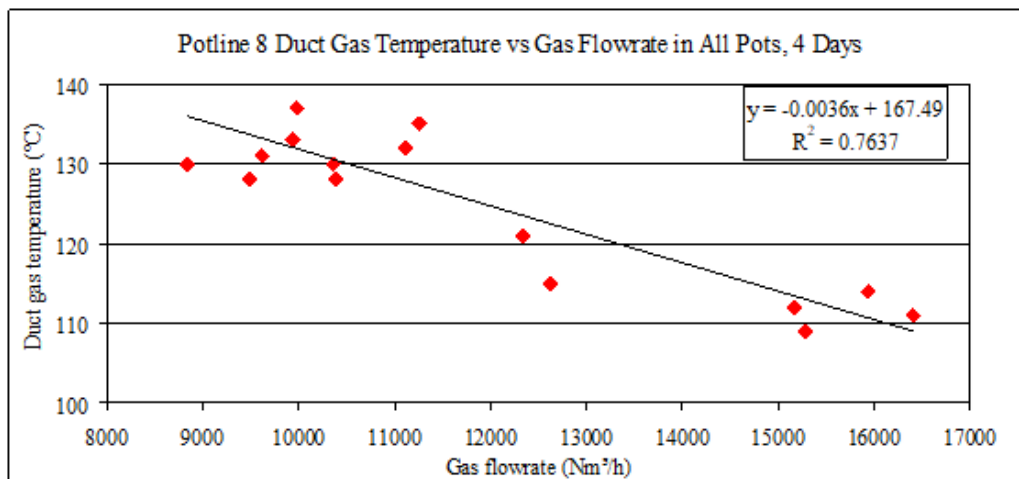


Figure 1. Measured gas temperature vs duct flowrate in EGA’s DX Potline (8 cells) at 385 kA [3].

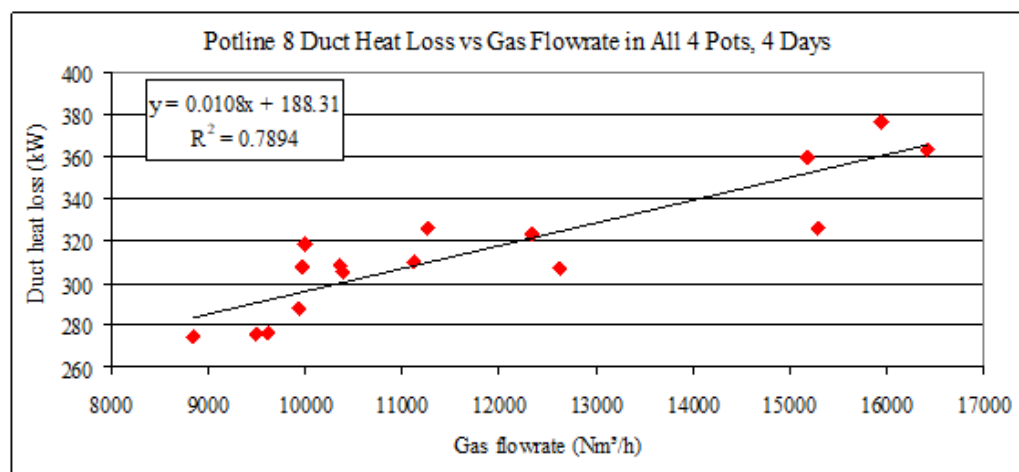


Figure 2. Measured heat loss vs duct flowrate in EGA’s DX Potline (8 cells) at 385 kA [3].

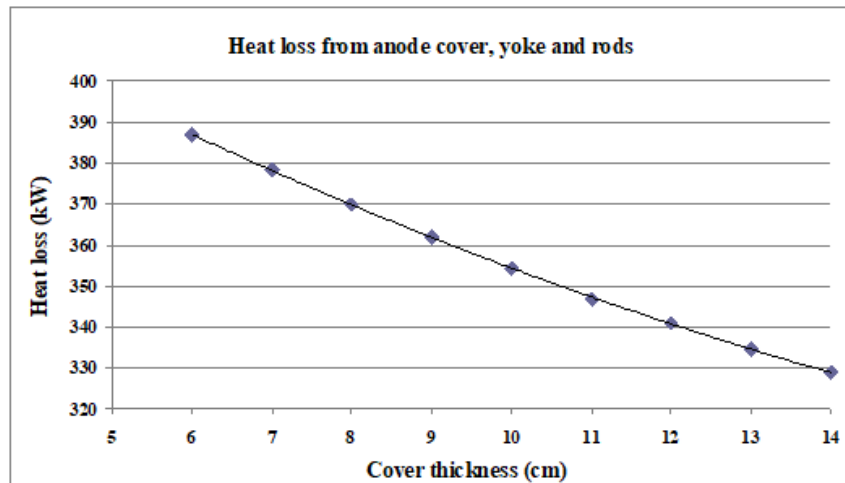
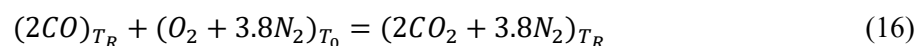
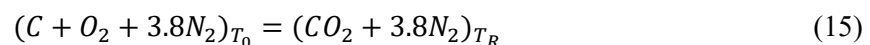


Figure 3. Heat loss from anode cover, yokes and rods in EGA’s DX+ demonstration cells at 440 kA, calculated with ANSYS model [7]. Extrapolated to 20 cm of anode cover, the heat loss would be 300 kW, 60 kW lower than at 9 cm of anode cover.

3.1 Sources of Waste Heat

The starting point of this energy balance is the determination of cell internal heat, which is the net heat inside boundaries of the cell, chosen for that purpose [7]. Internal heat is calculated from cell amperage and voltage inside the heat balance boundary, decreased by the heat absorbed by making aluminium. The total waste heat is equal to internal heat, because all the net heat in the cell must be lost through the boundaries. The distribution of the heat losses between the cathode and anode top must be calculated with mathematical models or measured. The result is that the top heat loss accounts for 40–50 % of internal heat. In [7], 42 % of internal heat is top heat loss, in [8] it is about 41 % (including the part of deckplate under the hood), in [6] it is about 46 % Including half of the deckplate under the hood). For the duct heat loss, the heat generation of anode oxidation and of CO burn must be added, but some of this may be already included in internal heat as in [7]. The measured duct heat loss in Figure 2 [3] accounts for 41 % of internal heat quoted in the paper, which does not include any carbon or CO burning. In [4], 74 % of top heat loss was through the duct, 18 % through the hoods and 6 % through the superstructure.

The amount of heat generated by the anode air-burn and carboxy reaction, and CO burn is best to be treated separately from internal heat since some of it is generated under the anode cover and part of it inside the hood. In any case all air has to be considered, including nitrogen, since the air enters at lower temperature than it leaves in the duct. Equations (15 and (16) give the reactions [7].



where:

T_0 Temperature of ambient air entering under the hood = 177 °C and

T_R Reaction temperature = 850 °C for carbon Equation (15) and 960°C for CO (Equation 16)

These two reactions are very exothermal and can generate a lot of heat. If for simplicity it is assumed that T_0 is 25 °C and $T_R = 960$ °C for both reactions, the Equation (15) generates 23.1 MJ/kg C and Equation (16) generates 5.75 MJ/kg CO. For 30 kg C/t Al excess carbon

oxidation, this gives 693.7 MJ/t Al = 193 kWh/t Al, equivalent to 24 kW. For 225 kg of CO/t Al, this gives 1294 MJ/t Al = 359 kWh/t Al, equivalent to 45 kW. These amounts of heat from carbon anode and CO burn are quite small in comparison to the total anode top heat loss.

4. Exergy Analysis

Exergy is the maximum amount of energy that can be converted into work, representing the quality grade of energy. Exergy is defined as energy times the Carnot efficiency, given Equation (17).

$$E_{xq} = Q \left(1 - \frac{T_0}{T} \right) \quad (17)$$

where:

E_{xq}	Exergy: maximum amount of heat convertible to useful work, kJ
Q	Total amount of heat transferred, kJ
T_0	Temperature downstream of heat recovery unit (“cold reservoir”), K
T	Heat source temperature (“hot reservoir”), K

The quality of electrolytic cell flue gas waste heat, quantified by its exergy value, is related to waste heat temperature. From Equation (17), the higher the flue gas temperature, the higher the exergy value of the waste heat, i.e., the greater the fraction that can be converted into work, meaning the higher the quality of the waste heat. Since the waste heat of electrolytic cell flue gas is relatively low in temperature, the fraction convertible to work is small, leading to a long investment payback period and low investment willingness.

Based on the analysis of flue gas waste heat sources, the main contributions are anode top heat loss, transferred from inside the cell, augmented by heat generated by carbon anode oxidation and CO combustion. Since the temperature inside the cell hood changes little during production, heat top heat transfer fluctuates minimally. When the total heat remains essentially constant, reducing the flue gas flow can increase the flue gas temperature, thereby increasing the exergy value of the flue gas waste heat. However, the minimum gas flow is determined by the requirement that no emissions exit the cell hoods.

In addition to flue gas waste heat, the cell also releases waste heat into the potroom through its sidewalls and the hood. This waste heat warms the potroom air from 30 °C to 45 °C, and when this air enters the exhaust system, it contributes to higher gas temperature and higher exergy.

5. Current Status of Flue Gas Waste Heat Recovery and Utilization

5.1 Approach Used

To estimate the exergy recoverable from cell flue gas, we follow the concept of calculating the waste heat in the flue gas from the total waste heat (= internal heat [7]), using the typical percentages quoted in the literature. The amount of heat entering under the hood through the anode cover is 40–45 % of the total waste heat. Most of this goes out with the flue gas, 35–40 % of the total waste heat, we will assume 36 % here [2]. Of course, using mathematical models would be more accurate for each technology, but here we want to show the principles.

The total waste heat, equal to internal heat calculated in [7], is (excluding excess anode carbon and CO burn, which are treated separately):

$$Q_{in} = (V_{cell} - V_{external} - V_{Al}) \cdot I \quad (18)$$

where:

Q_{in}	Internal heat = total waste heat, kW
V_{cell}	Cell voltage, V
$V_{external}$	External voltage from end of collector bars to anode rods just above the hood of next cell, V
V_{AL}	Voltage equivalent of enthalpy to make aluminium, V [7]
I	Cell current, kA

Data: $V_{cell} = 4.99$ V, $V_{external} = 0.250$ V, $V_{AL} = 2.05$ V (for current efficiency = 94 %, bath temperature = 960 °C, including some auxiliary processes), $I = 420$ kA [7]).

Results:

- $Q_{in} = 710$ kW.
- The anode top heat loss = 40–45 %; assuming 40 %; gives 284 kW.
- Assuming 36 % of total waste heat (internal eat) going out into the duct with the flue gas [2] gives 256 kW.
- Add to this the heat generated by air oxidation of excess anode consumption: 30 kg C/t Al generates 24 kW, and CO oxidation of 225 kg CO/t Al generates 45 kW (as calculated in Section 3.1). This gives the total waste heat = 325 kW in the flue gas. This is similar to Figure 2 at 12 700 Nm³/h gas flowrate.
- Assuming a temperature after heat recovery system of 100 °C (373 K). Then, according to Equation (17), exergy in the gas is 31.4 kW/cell for gas temperature T = 140 °C (413 K), 51.3 kW/cell for gas temperature T = 170 °C, and 68.6 kW/cell for gas temperature T = 200 °C (473 K).
- For a potline of 360 cells the total exergy is 11 MW, 19 MW and 25 MW for flue gas temperature of 140, 170 and 200 °C, respectively.

5.2 Industrial Examples

Flue gas waste heat from electrolytic cells is characterized by large gas flow, low quality, high dust content, and certain corrosiveness. At present, most cell flue gas waste heat is not utilized, with only a few smelters exploring recovery and utilization. The recovery and utilization of cell flue gas waste heat mainly focuses on heat utilization and power generation.

5.2.1 China

In China, the first waste heat power generation project in the aluminium industry, undertaken by Chalco. An industrial trial system was implemented and successfully connected to the grid. At full load, it can generate 3.2 GWh annually, equivalent to 365 kW, saving 393 tonnes of standard coal (1 t of standard coal = 8.139 MWh) and reducing CO₂ emissions by 1 284 tonnes. The flue gas waste heat power generation is fed back into the aluminium production system, reducing the manufacturing cost per tonne of aluminium – this belongs to power utilization.

Shuangyuan Aluminium flue gas waste heat utilization system uses the waste heat in exhaust flue gas from the cells to heat circulating water via a steam-water heat exchanger, supplying hot water for heating and domestic use. This achieves energy recovery and utilization, which is heat utilization, but is greatly affected by seasonal and regional factors.

5.2.2 Outside China

At Alcoa Deschambeault Quebec, Canada smelter, operating AP30 technology, the exergy analysis of waste heat was made in [9, 11]. In [9] the potline is analysed; at the time, the smelter had a production of 260 kt/a. The waste energy of the flue gas was estimated to be 2.94 MWh/t Al

and exergy in the cell duct was estimated to be 0.65 MWh/t Al (using gas temperature $T = 135\text{ }^{\circ}\text{C} = 408\text{ K}$ and $T_0 = 77\text{ }^{\circ}\text{C} = 350\text{ K}$). It was estimated that the whole smelter of 260 kt/a could recover 19 MW of heat from the duct gas. In [10] the exergy analysis is expanded to include anode production, electrolysis and cast house.

At ALBA, Bahrain, water-cooled heat exchangers (HEX) were installed in Potline 4 [11, 12]. Figure 4 shows a simplified diagram of the system. The main purpose was the cooling of flue gas for efficient dry scrubbing in GTC. Heat recovery was an additional benefit. It was estimated that 25 MW of heat could be recovered when the system would be operational in the entire potline. At the same time HEX reduced the power consumption on the main GTC. The recovered heat was used in large dry air coolers. Using the recovered heat in water desalination was also studied. Heat recovery also reduces carbon footprint [12].

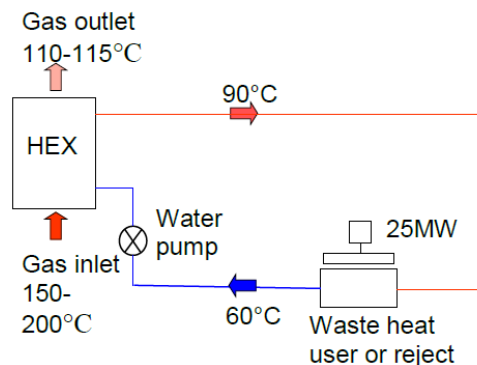


Figure 4. Simplified diagram of HEX heat recovery system in ALBA Potline 4 [12].

5.3 Usage of Recovered Heat from Flue Gas

Flue gas waste heat from cells can be used to produce saturated steam, which can then be used for power generation via saturated steam turbines or multi-stage flash steam power generation technology. This avoids the long-term working medium degradation issues found in Organic Rankine Cycle (ORC) units. Steam flash power generation operates under negative pressure, and the Guangzhou Institute of Energy Conversion, Chinese Academy of Sciences, has successful experience in this technology, with the power generation system at the Fengshun Geothermal Power Plant operating successfully for over 40 years.

In cold climates, such as Iceland and Norway, feasibility studies showed that the highest efficiency for the use of recovered waste heat from cell flue gasses is district heating of the nearby towns [13, 14].

6. Conclusions

Based on the analysis of flue gas flow and influencing factors in electrolytic cells, an energy and exergy analysis of the flue gas waste heat was made. The quality of the flue gas waste heat is quantified through heat exergy, and methods for improving its quality are proposed. It is suggested that gaps such as those at the cell hood have a significant impact on flue gas flow; by reducing gaps and improving sealing, flue gas flow can be reduced, flue gas temperature increased, and the exergy of the waste heat increased. Traditional methods of recovering flue gas waste heat have long investment payback periods due to the low temperature of the waste heat, and only a few companies use it for hot water production or demonstration power generation. By conducting an exergy analysis of the flue gas waste heat and proposing specific measures to improve its exergy value, this study provides important guidance for enhancing the energy utilization efficiency of electrolytic cells.

7. Acknowledgements

This project has been funded by the Guangxi Provincial Major Science and Technology Special Project titled "Research and Industrialization of Key Technologies for Utilizing Waste Heat from Electrolytic Cells", under Project Task Number: Guike AA2302319. The authors thank also Dr. Vinko Potocnik, ICSOBA Aluminium Electrolysis Subject Organizer, for thorough review and revision of this paper.

8. References

1. Yang Zhang, et al. Energy saving potential analysis and application practice of aluminium electrolysis cells [J]. *Nonferrous Metals* (Extractive Metallurgy), 2023, (08), 43–9 (in Chinese).
2. Haixiang Zhou. Exploring energy saving and emission reduction technologies for electrolytic aluminium production [J]. *China Metal Bulletin*, 2018, (3) (in Chinese).
3. Vinko Potocnik, Rawa Ba Raheem and Abdalla Alzarooni, Measurement of pot gas exhaust flowrate and heat loss, *Proceedings of 34th International Conference and Exhibition of ICSOBA*, Québec City, Canada, 3–6 October, 2016, *Travaux* 45, 671–681.
4. Haiam Abbas, Mark P Taylor, Mohammed Farid, John JJ Chen, The impact of cell ventilation on the top heat losses and fugitive emissions in an aluminium smelting cell, *TMS Light Metals* 2009, 551–556.
5. Zhuojun Xie, Weibo Li, Jian Lu, Zheng Liu and Hailong Guo, Relocation of a 400 kA potline – pot upgrade and energy saving roadmap, *Proceedings of the 41st International ICSOBA Conference*, Dubai, 5–9 November 2023, *TRAVAUX* 52, 1315–1324.
6. M.D. Gadd, B.J. Welch and A.D. Ackland, The effect of process operations on smelter cell top heat losses, *TMS Light Metals* 2000, 231–238.
7. Abdalla Al Zarouni, Lalit Mishra, Nadia Ahli, Marwan Bastaki, Amal Al Jasmi, Alexander Arkhipov and Vinko Potocnik, Energy and mass balance in DX+ cells during amperage increase, *Proceedings of 31st Conference of ICSOBA and XIX Conference "Aluminium Siberia"*, 4–6 September 2013, Krasnoyarsk, Russia, *Travaux* 42, 493–499.
8. Abdalla Zarouni et al. and Vinko Potocnik, Mathematical model validation of aluminium electrolysis cells at DUBAL, *TMS Light Metals* 2013, 597–602.
9. Cassandre Nowicki, Louis Gosselin and Carl Duchesne, Waste heat integration potential assessment through exergy analysis in an aluminium production facility, *TMS Energy Technology 2012: Carbon Dioxide Management and Other Technologies*, 165–172. <https://doi.org/10.1002/9781118365038.ch21>.
10. Ruijie Zhao, Cassandre Nowicki, Louis Gosselin, Carl Duchesne, Energy and exergy inventory in aluminium smelter from a thermal integration point-of-view, *International Journal of Energy Research*, 2016, 40, 1321–1338, <https://doi.org/10.1002/er.3508>.
11. Anders K. Sørhuus, Sivert Ose, Bent M. Nilsen, Possible use of 25 MW thermal energy recovered from the potgas at Alba Line 4, *TMS Light Metals* 2015, 631–636.
12. Anders Sørhuus, Håvard Olsen, Mikkel Sørum and Guillaume Girault, Cooling of pot gas enabling carbon footprint reductions, *TMS Light Metals* 2022, 531–536.
13. Martin Fleer et al., Heat recovery from the exhaust gas of aluminium reduction cells, *TMS Light Metals* 2010, 243–248.
14. Leo Blaer Haraldsson et al., Feasibility of a district heating system in Fjardabyggd using waste heat from Alcoa Fjardaal, *Energy Technology* 2019, TMS, https://doi.org/10.1007/978-3-030-06209-5_3

